JST: Engineering and Technology for Sustainable Development
Volume 35, Issue 3, July 2025, 052-060

Synthesis of Al_2O_3 - Y_2O_3 - SiO_2 Frit Additives by Combining Sol-Gel and Coprecipitation Methods for Advanced Ceramics SiAlON

Tran Van Cuong[1*], Ninh Duc Ha[1], Dang Quoc Khanh[2]
[1]*Institute of Chemistry and Material, Military Academy of Science and Technology, Ha Noi, Vietnam*
[2] *Hanoi University of Science and Technology, Ha Noi,Vietnam*
**Corresponding authors e-mail: trancuong.hhvl@gmail.com*

Abstract

Advanced SiAlON ceramics play a crucial role in high-temperature industries, such as aluminum smelting, due to their superior properties, including high thermal stability, excellent thermal shock resistance, and anticorrosive behavior. In the study, Al_2O_3-Y_2O_3-SiO_2 frits (2A4Y3S and 2A5Y2S) were synthesized via sintering, and the dynamic phase formation of these materials was investigated. To lower the sintering temperature, Y_2O_3 and Al_2O_3 particles were synthesized using a co-precipitation method, employing $Al(NO_3)_3{\cdot}9H_2O$ and $Y(NO_3)_3{\cdot}6H_2O$ in an NH_4OH solution. Meanwhile, SiO_2 was prepared via the sol-gel method using Na_2SiO_3 as the precursor and HCl as a catalyst. The effects of synthesis conditions on the formation of 2A4Y3S and 2A5Y2S frits via sintering were systematically analyzed using X-ray diffraction (XRD), differential thermal analysis (DTA), and scanning electron microscopy (SEM). The optimal synthesis conditions for 2A4Y3S were achieved by melting at 1200 °C for 5 hours. At 1000 °C, 2A4Y3S exhibited a fully amorphous structure, with crystallization occurring in the temperature range of 1100 °C to 1200 °C. In contrast, the optimal synthesis conditions for 2A5Y2S were obtained by melting at 1300 °C for 5 hours. This material remained fully amorphous at 1100 °C, with crystallization occurring between 1200 °C and 1300 °C. Notably, the crystallization temperatures observed in this study were significantly lower than those required for conventional solid-state reaction methods used in the preparation of advanced ceramics.

Keywords: Y_2O_3 - Al_2O_3 - SiO_2; frit; ceramics; SiAlON.

1. Introduction

Advanced ceramics such as SiAlON materials are widely used in industries requiring high-temperature operations [1], thanks to their outstanding properties, including high elastic modulus, excellent thermal shock resistance, high hardness, high load deformation temperature, low thermal expansion, and durability in corrosive environments (acids, bases, salts, molten metals) [2]. The anticorrosive behavior in molten metal environments and their resistant capabilities to oxidation at high temperatures up to 1500 °C enable them to be an excellent candidate used in high temperature industry [3]. As a result, they are key materials for producing components in molten metal casting, such as casting tubes, filters, temperature sensor protection tubes, and ceramic tubes for induction furnaces [4]. However, synthesis of advanced SiAlON ceramics is challenging due to the high temperature sintering up to 1900 °C or higher [5]. Conventional solid-state reaction method is used to synthesis SiAlON ceramics required sintering temperature of 1700 °C [6]. Many attempts have been made to reduce the synthesis temperature of SiAlON materials by adding some additives, and/or using the sol-gel method [7].

Recently, mixed oxides Y_2O_3 - Al_2O_3 - SiO_2 of different compositions (namely 2A4Y3S and 2A5Y2S frits) can be used as effective additives to reduce the sintering temperatures and to enhance the mechanical properties of SiAlON ceramics [8, 9]. Additionally, such additives also influence the densification level and structure of the ceramic, enabling the advanced applications [10, 11]. Therefore, extensive methods have been developed to prepare 2A4Y3S and 2A5Y2S frits such as sol-gel Pechini, sol-gel, co-precipitation, hydrothermal methods, combustion combined with microwave processes, peptization of oxalate gels, acid acetate-based gels, and melting routes [12, 13]. Among them, the sol-gel melting method is a fast, simple approach that is suitable for large-scale production of frits. The mixed metal oxides, namely 2A4Y3S and 2A5Y2S frits are commonly used as raw materials for the synthesis of SiAlON. However, it is challenging in synthesis of crystalline 2A4Y3S and 2A5Y2S frits for application in preparation of advanced SiAlON. Furthermore, understanding the phase transformation of the frits during thermal treatment is also important in optimization of the fabrication of advanced ceramic SiAlON.

ISSN 2734-9381
https://doi.org/10.51316/jst.183.etsd.2025.35.3.7
Received: Feb 14, 2025; revised: Apr 23, 2025
accepted: Jun 3, 2025

In this study, the crystalline 2A4Y3S and 2A5Y2S frits were prepared by combination of sol-gel and co-precipitation products to create a homogeneous oxide mixture, followed by melting and rapid cooling with water at room temperature. The method enhances the homogeneity of the 2A4Y3S, 2A5Y2S frits, and significantly reduces the melting temperature, resulting in high quality frits. Additionally, we also focus on investigating the effects of synthesis conditions on the properties of 2A4Y3S and 2A5Y2S frits.

2. Experiments

2A4Y3S and 2A5Y2S frits were prepared with $Al(NO_3)_3.9H_2O$ (Sigma-Aldrich; 99.8%), $Y(NO_3)_3.6H_2O$ (Sigma-Aldrich; 99.8%) and Na_2SiO_3 (Sigma-Aldrich; 25.5 - 28.5% SiO_2) as raw materials. The synthesis process of 2A4Y3S and 2A5Y2S frits are shown in Figure 1.

Typically, SiO_2 powders were prepared by a sol-gel method. At the beginning of the synthesis process, Na_2SiO_3 solution was continuously stirred using a magnetic stirrer at temperature of approximately 80 °C. Then, 0.5 M HCl was gradually added to control the pH of solution to be about 9. It was emphasized that the gelation process occurred rapidly when Na_2SiO_3 came into contact with HCl (1).

$$Na_2SiO_3 + H_2O + HCl \rightarrow Si(OH)_4 + 2NaCl \quad (1)$$

Therefore, it was essential to ensure that the entire sample was well mixed during the HCl addition to achieve a homogeneous gel product. The resulting product was then dried at 90 °C overnight to obtain the dried gel. Finally, after washing multiple times with ethanol and distilled water, the sample was ground to obtain SiO_2 powders.

Coprecipitation method was conducted with an NH_3 solution as the precipitant to prepare Al_2O_3 and Y_2O_3 powders. Specifically, 1 M solutions of yttrium and aluminum salts were first prepared and then mixed. Next, a small amount of aqueous ammonia was added dropwise to the mixture until a pH of approximately 8.3. This solution was aged with mild agitation for approximately 30 minutes at 80 °C. The precipitates formed during the aging process were collected by filtration. They were then washed multiple times with alcohol and distilled water to remove impurities and dried at 100 °C until completely dry. Finally, they were finely ground with an agate mortar and calcined at an appropriate temperature to form Al_2O_3, and Y_2O_3 oxides (Fig. 1).

The prepared Al_2O_3, Y_2O_3, and SiO_2 powders were then mixed in isopropanol according to pre-calculated mass ratios (Table 1). The mixture was finely milled using a planetary ball-mill for 0.5 hours and then completely dried at approximately 100 °C. The resulting powder mixture was transferred into a platinum crucible for melting in an electric furnace. The melting process was conducted at 1200 °C or 1300 °C for 5 hours, with a heating rate of 10°C/min. After that, it was rapidly cooled with water to obtain 2A4Y3S and 2A5Y2S frits fragments. These frit fragments, with sizes of several millimeters, were finally milled in ethanol using a ball-mill to achieve frit powders of less than 5 μm in size for next investigation.

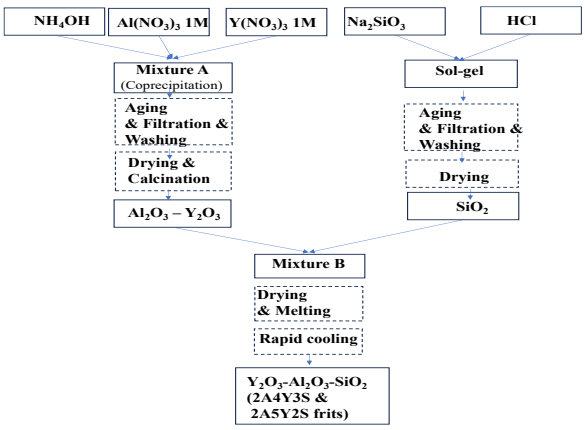

Fig. 1. Synthesis process of 2A4Y3S and 2A5Y2S frits

Table 1. Composition of 2A4Y3S, 2A5Y2S frits, commercial type P1 and preparation methods.

No	Name	Sample	Composition, wt%			Prepared Method
			Al_2O_3	Y_2O_3	SiO_2	
1	Q	2A4Y3S	2.52	4.15	3.33	Sol-gel
2	P	2A5Y2S	2.21	5.35	2.44	Sol-gel
3	Commercial type	P1	2.51	4.32	3.07	Mixed oxides

The commercial product noted as P1 was also used for comparison. All the samples are summarized in table 1. The mixture from Al_2O_3, Y_2O_3, and SiO_2 powders were finely milled using a planetary ball-mill for 0.5 hours and then completely dried at approximately 100 °C. The resulting powder mixture was transferred into a platinum crucible for melting in an electric furnace. After that, it was rapidly cooled with water to obtain commercial type P1 frits.

The glass transition temperature (T_g), crystallization peak temperature (T_c), and crystal structures of the samples were analyzed using differential thermal analysis (DTA) (Linseis, STA PT 2400, Germany) and X-ray powder diffraction (XRD) (Bruker, Germany). The morphology of the synthesized samples was examined by scanning electron microscopy (SEM) (HITACHI S-4800, Japan).

The hardness of the samples was measured using a ZwickRoell apparatus (Germany). For each sample,

five measurements were performed under a 50 g load for 10 seconds, and the average value was recorded. The densities and porosities of the samples were determined according TCVN 6530-3:2016, with ten measurements conducted for each sample, and the average value was reported. The thermal expansion coefficients of the glass samples were measured using a Netzsch apparatus (Germany) with a heating rate of 5 K/min up to 700 °C.

3. Results and Discussion

3.1. Phase Transition Temperatures of the 2A4Y3S and 2A5Y2S Frits

In the synthesis of advanced ceramic, the phase transition temperature and the crystallization temperature are very important thus, we used DTA to investigate such properties of the 2A4Y3S and 2A5Y2S frits. All the DTA measurements were carried out in air ambient. The DTA results of the 2A4Y3S and 2A5Y2S frits are presented in Fig. 2.

The T_g of the 2A4Y3S sample was found to be 850 °C. This value is lower than that of the sample prepared by a mixing method. The first crystallization peak (T_{c1}) occurred at 1120 °C, while the second crystallization peak (T_{c2}) was found at approximately 1284 °C. Therefore, the crystallization process of 2A4Y3S occurs strongly in the temperature range from 1120 °C to 1284 °C. The eutectic temperature was observed at around 1302 °C. Note that in the solid-state reaction method, the glass transition temperature (T_g) and the crystallization peak temperature (T_c) was 909 °C and 1209-1378 °C, respectively [14]. Here, the 2A4Y3S sample has much lower T_g and T_c, indicating the advantages of the frits.

Similar to the 2A4Y3S sample, the T_g of the 2A5Y2S sample was found to be 897 °C (Fig. 2(b)). The first crystallization peak (T_{c1}) occurred at 1192 °C, while the second crystallization peak (T_{c2}) was found at approximately 1338 °C. Therefore, the crystallizatio n process of 2A5Y2S occurs strongly in the temperature range from 1192 °C to 1338 °C. The eutectic temperature was observed at around 1375 °C. The measured glass transition temperatures were lower than the values reported in the published literature. It should be emphasized that in the same glass system, a lower glass transition temperature suggests more favorable conditions for crystallization behavior to occur. Such findings suggest the advantages of the synthesis process for the synthesis of 2A4Y3S and 2A5Y2S frits for the preparation of advanced ceramic SiAlON [15].

From Table 2, it can be seen that both 2A4Y3S and 2A5Y2S frits have lower T_g, T_{c1}, T_{c2} and T_e temperatures than those of the commercial produce (sample P1). This is explained by the fact that the sol-gel method produces oxides in amorphous form, so the melting temperature is lower than the method of mixing oxides from crystalline form. Therefore, using our prepared frits for the fabrication of SiAlON is more advantage in formation of homogenous materials.

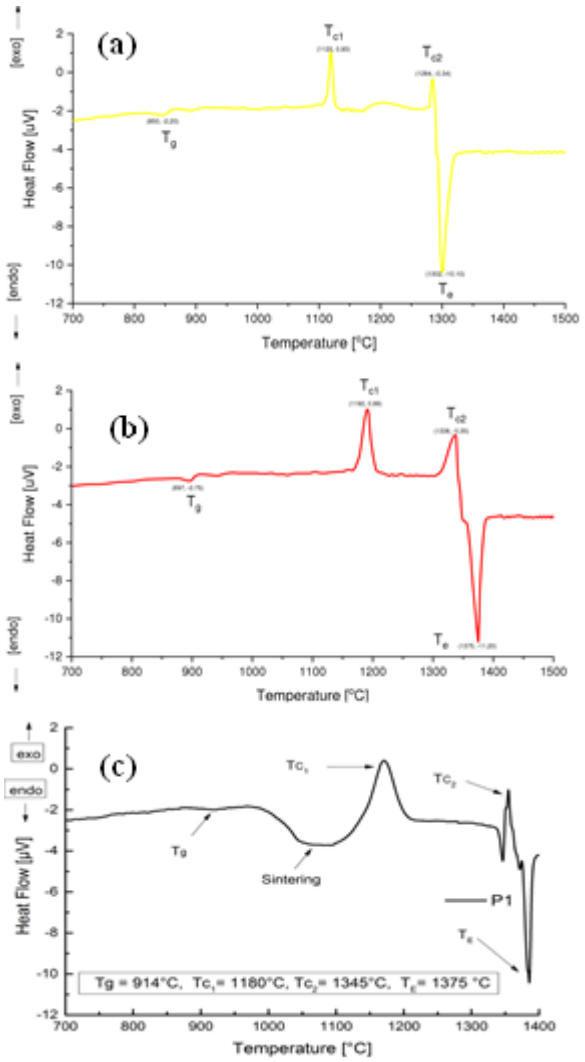

Fig. 2. DTA data of the synthesized frits: (a) 2A4Y3S from sol - gel method; (b) 2A5Y2S from sol - gel method; (c) Commercial type P1.

Table 2. DTA analysis results of 2A4Y3S and 2A5Y2S frits

No	Sample	T_g (°C)	T_{C1}	T_{C2}	T_e (°C)
1	2A4Y3S	850	1120	1284	1302
2	2A5Y2S	897	1192	1338	1375
3	Commercial type P1	914	1180	1345	1375

3.2. Effect of Temperature on the Crystallization Process of Al_2O_3 - Y_2O_3 - SiO_2 Frit

The prepared 2A4Y3S frits were fired at 800 °C, 900 °C, 1000 °C, 1100 °C, and 1200 °C for 0.5 h to investigate the effect of melting temperature on the crystal growth and the phase composition. Phase composition of the 2A4Y3S frit samples fired at different temperatures was determined by XRD analysis, and the data are shown in Fig. 3.

As shown in Fig. 3, no significant peak was observed in the sample fired at 800 °C, except for a broad peak at around 25°, indicating a completely amorphous structure. The result is consistent with the DTA analysis, where the glass transition temperature occurred at 850 °C.

However, in the sample fired at 900 °C, the mullite ($3Al_2O_3.2SiO_2$) crystals started to form at peak *2θ equal 25.8°* with a weak intensity. Further increase the fired temperature to 1000 °C, mullite phase crystals had a stronger peak at *2θ equal 25.8°*. The mullite phase crystals also formed new peaks at *2θ equal 16.5°* and *35.9°*. Yttrium disilicate ($Y_2O_3.2SiO_2$) phase started to appear at peak *2θ equal 29.4°* and weak peak intensity.

When the fired temperature increased to 1100 °C, the mullite phase crystal continued to form new peaks at *2θ equal 32.6°, 40.8°,* and *61.0°*. The intensities of the mullite crystal phase increases at the peak *2θ equal 16.5°, 25.8°,* and *35.9°*. Such results indicated the growth of mullite crystals. The yttrium disilicate phase also formed new peaks at *2θ equal 27.6°, 32.6°,* and *39.6°*. The peak intensity of the yttrium disilicate crystal phase increases at *2θ equal 29.4°*. Therefore, the 2A4Y3S frit fired at 1000 °C and 1100 °C composed of two phases, the mullite and the yttrium disilicate phase.

When the fired temperature increased to 1200 °C, the mullite crystal phase (JCPDS 00-015-0776) continued to form new peaks at *2θ equal 58.1°,* and *71.0°*. The peak intensity of the mullite crystal phase increases at the peak *2θ equal 16.5°, 25.8°, 32.6°, 35.9°, 40.8°, 61.0°*. The yttrium disilicate phase (JCPDS 01-076-9320) formed new peaks at *2θ equal 27.6°, 32.6°,* and *39.6°*. The peak intensities of the yttrium disilicate crystalline phase increases at *2θ equal 19.1°, 44.1°,* and *47.7°*. At this temperature, the corundum (Al_2O_3) crystalline phase (JCPDS 01-076-7775) appeared at the peaks *2θ equal 25.8°, 35.9°, 42.7°, 52.3°, 57.3°, 68.0°,* and *77.0°*.

From this observation, it can be concluded that the crystalline phases in the 2A4Y3S frit sample formed in the following order: mullite, yttrium disilicate and corundum. The formation of the first mullite crystal phase is due to the lowest melting point of SiO_2 (1710 °C), followed by Al_2O_3 (2072 °C) and finally the highest melting point is Y_2O_3 (2425 °C). The yttrium disilicate phase formed later possibly due to the low melting point of SiO_2, which is an agent to promote the reaction to form $Y_2O_3.2SiO_2$ to occur faster. The corundum crystal phase formed last because it was formed from Al_2O_3 oxide with a high melting point. The peak intensities of these crystalline phases remained stable above 1150 °C. Maximum crystallization was observed between 1150 to 1200 °C, consistent with the differential thermal analysis (DTA) results. Therefore, 1200 °C was selected as the optimal temperature for synthesizing the 2A4Y3S frit.

The calculation Highscore Plus software shown that 2A4Y3S frit fired for 0.5 hours at 1200 °C have 42,4% mullite; 35,9% yttrium disilicate; 9,7% corundum; and 12% glass. Such composition is effective for the preparation of advanced ceramic SiAlON.

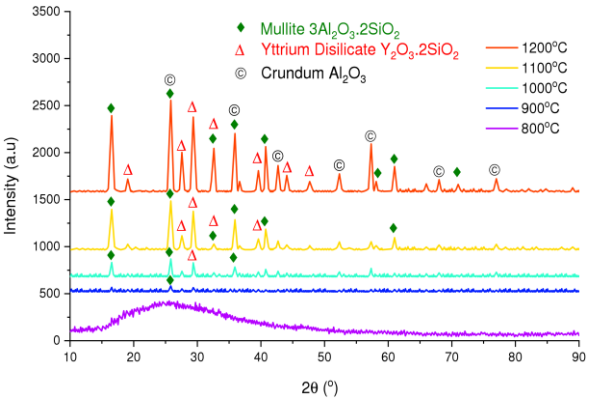

Fig. 3. XRD patterns of the 2A4Y3S frit fired for 0.5 hours at (a) 800 °C, (b) 900 °C, (c) 1000 °C, (d) 1100 °C, and (e) 1200 °C.

The melting process of the 2A5Y2S frit was conducted at 900 °C, 1000 °C, 1100 °C, 1200 °C, and 1300 °C to investigate the effect of temperature on phase composition and crystallization. The phase composition of the 2A5Y2S frit samples was analyzed using X-ray diffraction (XRD), as shown in Fig. 4.

The XRD patterns exhibit similar characteristics to those of the 2A4Y3S frit. At 900 °C, only an amorphous peak was observed. At 1000 °C, yttrium disilicate crystals began to form, with a diffraction peak at *2θ equal 28.8°*. At this temperature, yttrium silicate ($Y_2O_3.SiO_2$) crystals also appeared at *2θ equal 30.9°*.

At 1100 °C, the intensity of the yttrium disilicate increase at the peak *2θ equal 29.4°*, while the peak of yttrium silicate appears at *2θ equal 30.9°*. Additionally, new yttrium disilicate peak was observed at *2θ equal 32.6°*. As the temperature increased to 1200 °C, the yttrium disilicate phase developed additional peaks at *2θ equal 27.6°,* and *47.5°*. The yttrium silicate phase also exhibited new peaks at *2θ equal 23.1°, 26.1°, 42.8°*, and *52.8°*.

The intensities of the yttrium disilicate increases at the peaks *2θ equal 29.4°,* and *32.6°*, while the peaks of yttrium silicate appears at *2θ equal 29.4°,* and *30.9°*.

At 1300 °C, the yttrium disilicate crystalline phase (JCPDS 01-076-9320) exhibited additional peaks at *2θ equal 19.1°, 39.6°, 44.1°*, and *58.1°*. The yttrium silicate phase (JCPDS 01-084-4286) formed new peaks at *2θ equal 14.9°, 16.1°*, and *61.0°*. The intensities of the yttrium disilicate peaks increases at *2θ equal 27.6°, 29.4°, 32.6°*, and *47.5°*. Similarly, the yttrium silicate phase exhibited increased peak intensities at *2θ equal 23.1°, 26.1°, 29.4°, 30.9°, 42.8°*, and *52.8°*.

At this temperature, the corundum crystalline phase (JCPDS 01-076-7775) appeared at *2θ equal 25.0°, 34.8°, 36.6°, 42.8°, 52.8°, 57.3°, 68.0°, 77.0°*, and *89.0°*. Additionally, the yttrium aluminum garnet ($3Y_2O_3.5Al_2O_3$) phase (JCPDS 00-033-0040) was detected at *2θ equal 17.4°, 27.6°, 29.4°, 32.6°, 41.4°, 47.5°, 52.8°, 54.7°, 62.0°, 72.0°, 87.0°,* and *89.0°*.

These results indicate that the crystalline phases formed in the following order: yttrium disilicate, yttrium silicate, corundum, and yttrium aluminum garnet. This sequential formation is attributed to the increasing melting temperatures of SiO_2, Al_2O_3, and Y_2O_3 oxides, which require progressively higher energy to form $Y_2O_3{\cdot}2SiO_2$, $Y_2O_3{\cdot}SiO_2$, Al_2O_3, and $3Y_2O_3{\cdot}5Al_2O_3$ bonds.

The peak intensities of these crystalline phases stabilized above 1200 °C, with maximum crystallization occurring between 1250 °C and 1300 °C, consistent with differential thermal analysis (DTA) results. Therefore, 1300 °C was selected as the optimal temperature for synthesizing the 2A5Y2S frit. From Highscore Plus software confirmed that the 2A5Y2S frit fired at 1300 °C for 0.5 hours consists of 45.3% yttrium disilicate, 19.7% yttrium silicate, 15.0% corundum, 10.0% yttrium aluminum garnet, and 10.0% glass.

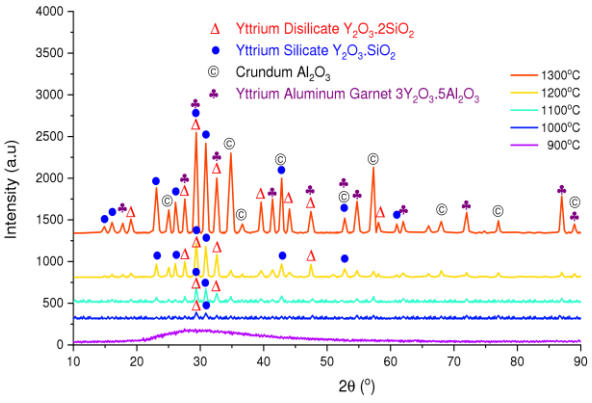

Fig. 4. XRD patterns of 2A5Y2S frit fired for 0.5 hours at(a) 900 °C, (b) 1000 °C, (c) 1100 °C, (d) 1200 °C, and (e) 1300 °C.

For the commercial product (sample P1), the melting process was conducted at 1200 °C for 0.5 hours to investigate its phase composition and crystallization behavior. As shown in Fig. 5, at 1200 °C, mullite and yttrium disilicate phases form, while cristobalite (SiO_2) remains. The presence of cristobalite may destabilize the frit's properties due to its potential phase transformation into quartz or tridymite. As compared with the 2A4Y3S and 2A5Y2S frits prepared by sol-gel methods, the commercial product has an unknown phase, meaning that the frits prepared by combining sol-gel and coprecipitation methods are advantages for ceramic preparation.

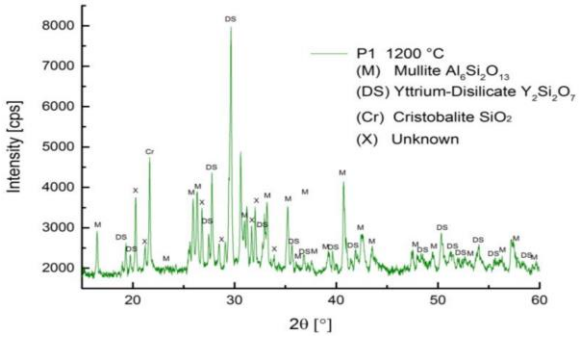

Fig. 5. XRD pattern of commercial P1 frit fired for 0.5 hours at 1200 °C.

3.3. Effect of Melting Duration on the Phase Composition of the Prepared Frits

Melting duration influences the phase formation and composition of frits. Therefore, 2A4Y3S frit samples were melted at 1200 °C for 5 and 10 hours to investigate changes in phase composition. The XRD data of the 2A4Y3S samples melted for 5 and 10 hours are shown in Fig. 6.

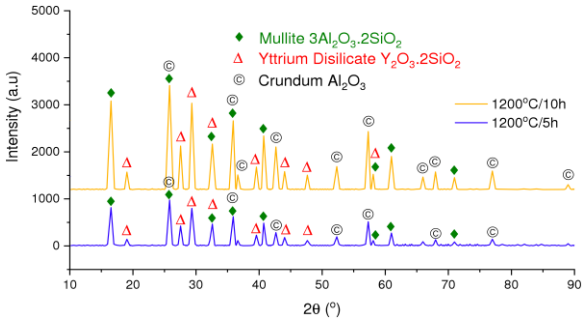

Fig. 6. XRD patterns of the 2A4Y3S frit melted at 1200 °C for 5 hours and 10 hours.

When held at 1200 °C for 10 hours, the intensity of the mullite crystalline phase (JCPDS 00-015-0776) increases at the peak *2θ equal 16.5°, 25.8°, 32.6°, 35.9°, 40.8°, 58.1°, 61.0°,* and *71.0°*. At this temperature, the yttrium disilicate phase (JCPDS 01-076-9320) exhibited further crystallization, with the

formation of a new weak peak at *2θ equal 58.1°*. The peak intensities of the yttrium disilicate crystalline phase increases at *2θ equal 19.1°, 27.6°, 29.4°, 32.6°, 39.6°, 44.1°,* and *47.7°*. The corundum crystalline phase (JCPDS 01-076-7775) also exhibited further crystallization, with new peaks forming at *2θ equal 36.6°, 66.0°,* and *89.0°*. The peak intensities of corundum increases at *2θ equal 25.8°, 35.9°, 42.7°, 52.3°, 57.3°, 68.0°,* and *77.0°*.

The XRD analysis confirms that the intensities of peaks corresponding to mullite, yttrium disilicate, and corundum in the sample melted at 1200 °C for 10 hours are significantly higher than those in the sample melted for 5 hours. These results indicate that increasing the melting duration enhances the crystallinity of the ceramic.

Similarly, the 2A5Y2S frit samples were melted at 1300 °C for 5 a nd 10 hours to examine changes in phase composition. The XRD data of the 2A5Y2S samples melted for 5 and 10 hours are shown in Fig. 7. When held at 1300 °C for 10 hours, the intensity of the yttrium disilicate crystalline phase (JCPDS 01-076-9320) increases at the peak *2θ equal 19.1°, 27.6°, 29.4°, 32.6°, 39.6°, 44.1°, 47.5°,* and *58.1°*. The peak intensities of the yttrium silicate crystalline phase (JCPDS 01-084-4286) increases at *2θ equal 14.9°, 16.1°, 23.1°, 26.1°, 29.4°, 30.9°, 42.8°, 52.8°,* and *61.0°*. The corundum crystalline phase (JCPDS 01-076-7775) exhibited further crystallization, with a new peak appearing at *2θ equal 66.0°*. The peak intensities of corundum increases at *2θ equal 25.0°, 34.8°, 36.6°, 42.8°, 52.8°, 57.3°, 68.0°, 77.0°,* and *89.0°*.

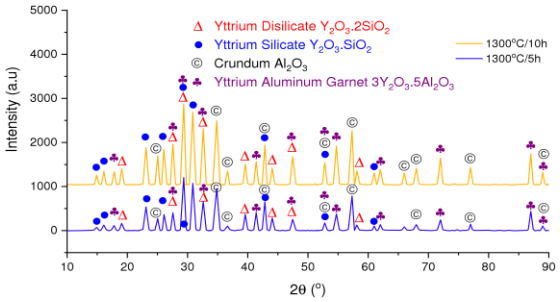

Fig. 7. XRD patterns of the 2A5Y2S frit melted at 1300°C for (a) 5 hours and (b) 10 hours.

The peak intensity of the yttrium aluminum garnet crystalline phase (JCPDS 00-033-0040) continued to increase at peaks *2θ equal 17.8°, 27.6°, 29.4°, 32.6°, 41.4°, 47.5°, 52.8°, 54.7°, 62.0°, 72.0°, 87.0°,* and *89.0°*.

The XRD analysis confirms that the intensities of peaks corresponding to yttrium disilicate, yttrium silicate, corundum, and yttrium aluminum garnet in the sample melted at 1300 °C for 10 hours are significantly higher than those in the sample melted for 5 hours. These results indicate that increasing the melting duration enhances the crystallinity of the ceramic.

The SEM is an advanced method to study the morphology of the prepared samples. Therefore, in this study, the change in the morphology of the 2A4Y3S samples over the melting durations (0.5, 5, and 10 hours) was observed by SEM as shown in Fig. 8. The results show that the 2A4Y3S sample melted at 1200 °C in 10 hours containing phase crystals distributed and exhibited a higher degree of crystallization compared to the sample at 0.5 and 5 hours. Fine particle structure was observed in the samples melted for 5 and 10 hours.

The formation of this fine microstructure led to the appearance of secondary crystallization peaks during the DTA analysis of the 2A4Y3S frit. The SEM images indicate that the structure of this sample comprises mullite, yttrium disilicate, and corundum. Surface of the prepared samples are very smooth, and the sample composed of nanoparticles of less than 15 nm in size. Note that during the frit fabrication process, no sample pressing was performed; thus, the obtained samples are entirely natural. However, they exhibit good densification with a uniform nanostructure, making them suitable for advanced ceramic applications.

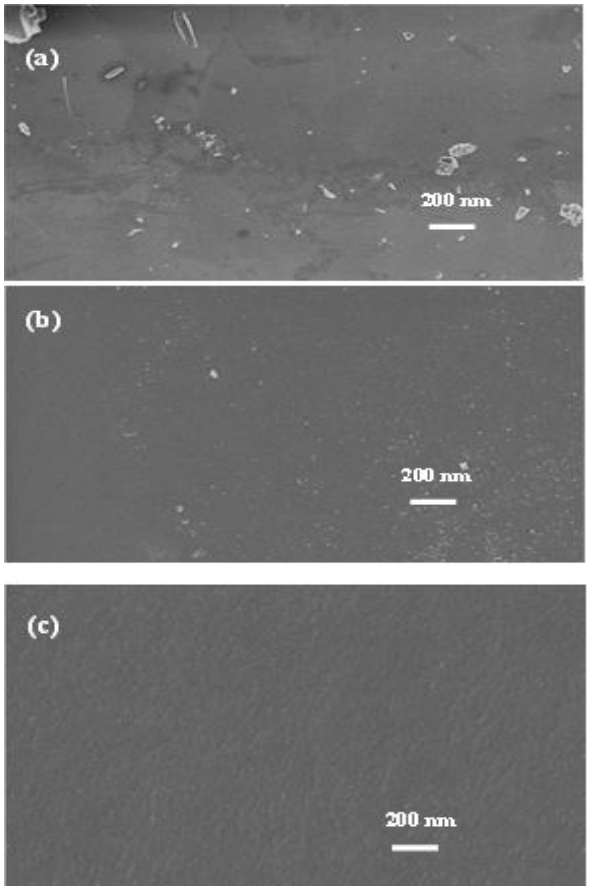

Fig. 8. SEM image of 2A4Y3S frit melted at 1200 °C for (a) 0.5 hours, (b) 5 hours, and (c) 10 hours.

The change in the morphology of the 2A5Y2S samples over the melting durations (0.5, 5, and 10 hours) was also observed through the SEM images as shown in Fig. 9. SEM images indicate that the prepared samples are highly densification. The samples are composed of fine nanoparticles. With the increase of melting duration, the size of nanoparticles increased due to the grain growth. The SEM results show that the 2A5Y2S sample melted at 1300 °C for 10 hours contains phase crystals distributed and exhibited a higher degree of crystallization compared to the sample at 0.5 and 5 hours. The formation of this fine microstructure observed by the SEM images is consistent with the DTA analysis of the 2A5Y2S frit, confirming the appearance of secondary crystallization peaks during the melting processes. The SEM images indicate that the structure of this sample comprises yttrium disilicate, yttrium silicate, corundum, and yttrium aluminum garnet.

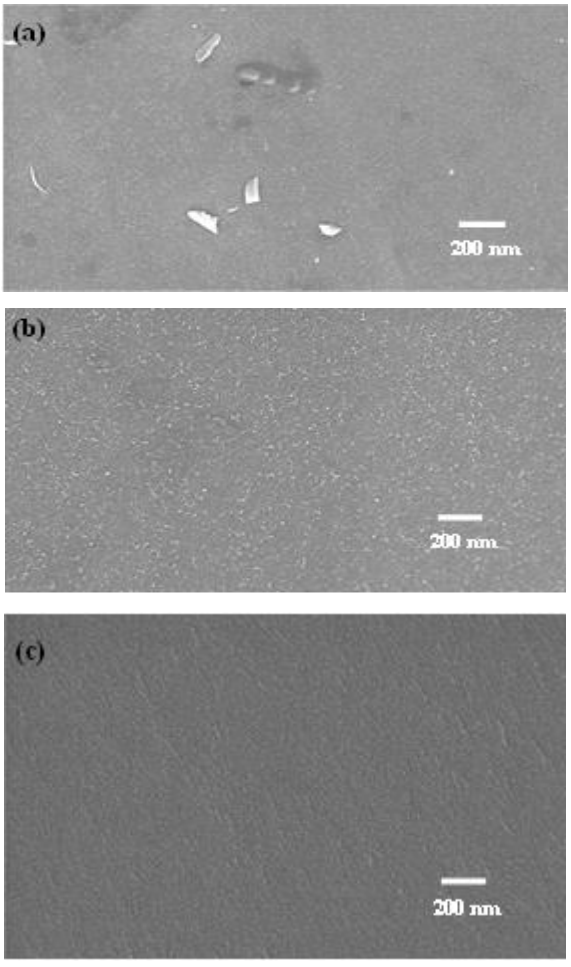

Fig. 9. SEM image of 2A5Y2S frit melted at 1300 ºC for (a) 0.5 hours, (b) 5 hours, and (c) 10 hours.

In addition, the change in the morphology and composition of the 2A4Y3S and 2A5Y2S frits over the melting durations of 5 hours was also observed through EDX Mapping as shown in Fig. 10 (a), and (b), respectively. Results demonstrate that the prepared samples are homogenous, and the materials composed of Al, Si, Y, and O consistently with the starting composition.

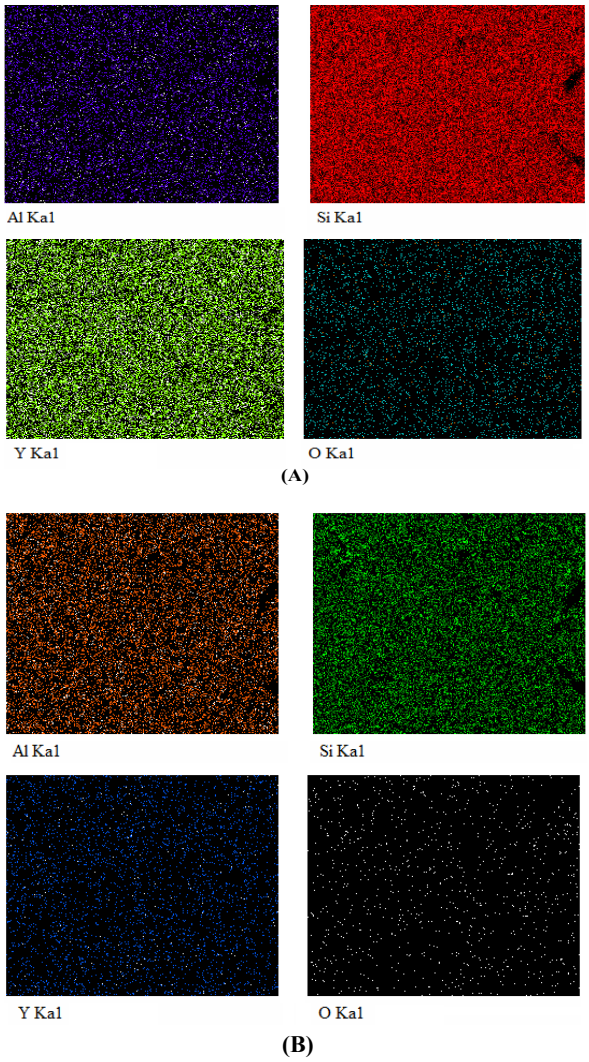

Fig. 10. EDX mapping of the frits melted for 5 hours: 2A4Y3S at (a) 1200 ºC, 2A5Y2S at (b) 1300 ºC

3.4. Physical Properties of the Prepared Frits

Various quantitative techniques were employed to analyze different frit samples, including 2A4Y3S, 2A5Y2S, and the commercial P1 frits, to determine their physical properties such as density, hardness, and thermal conductivity. The summarized results are presented in Table 3.

Table 3. Mechanical, physical, thermal properties of 2A4Y3S, 2A5Y2S, and commercial type P1 frits

No	Sample	Mechanical properties: Hardness (HV)	Physical properties		Thermal properties	
			Density (g/cm^3)	Porosity (%)	Coefficient of thermal expansion 100-700 °C (10^{-6} K^{-1})	Thermal conductivity (W/mK)
1	2A4Y3S	900.2	3.04	0.10	4.29	0.492
2	2A5Y2S	994.6	3.25	0.08	4.30	0.493
3	Commercial type P1	852.5	2.81	0.15	4.36	0.520

The 2A5Y2S frit exhibited the highest bulk density (3.25 g/cm^3), followed by 2A4Y3S (3.04 g/cm^3), and commercial P1 frit (2.81 g/cm^3). The higher bulk density of the 2A5Y2S frit is possibly due to its synthesis via the sol-gel method, resulting in amorphous oxides, lower melting temperature, and improved aggregation. By using our synthesis method, the bulk density of the 2A4Y3S frit is improved 8.2% and T_g, T_{c1}, T_{c2}, T_e is smaller as compared with the commercial P1 frit while the composition of 2A4Y3S frit is almost equal to the composition of commercial P1 frit. The 2A4Y3S, and 2A5Y2S samples exhibited higher bulk densities compared to the commercial P1 frit, attributed to their higher Y_2O_3 content, which also correlates with an increased melting temperature. Additionally, the measured porosities of the 2A4Y3S, 2A5Y2S, and P1 frit samples were 0.10%, 0.08%, and 0.15%, respectively. The 2A5Y2S frit displays the lowest porosity. The observed trend of decreasing porosity with increasing density indicates that a higher degree of compaction leads to reduced porosity.

Regarding the hardness, the values recorded for 2A4Y3S, 2A5Y2S, and P1 frits were 900.2, 994.6, and 852.5 HV, respectively. The 2A5Y2S frit demonstrated the highest hardness, which aligns with the trend of increasing densification and compaction, leading to enhanced mechanical strength.

Thermal conductivity values of the 2A4Y3S, 2A5Y2S, and P1 frits were 0.492, 0.493, and 0.520 W/mK, respectively. The thermal conductivity of 2A4Y3S frit is as same as that of 2A5Y2S frit because the density expressed through porosity of the two samples is almost the same.

The thermal expansion coefficients of the 2A4Y3S, 2A5Y2S, and P1 frits were 4.29, 4.30, and 4.36×10^{-6} K^{-1}, respectively. The nearly identical and lower thermal expansion coefficients of the 2A4Y3S, and 2A5Y2S frits compared to that of the P1 frit suggest superior thermal stability. In particular, the 2A5Y2S frit synthesized via the sol-gel method showed excellent properties. Therefore, such parameters confirm that the prepared 2A5Y2S frit is excellent for preparation of advanced ceramic as compared to 2A4Y3S or the commercial product.

4. Conclusion

In conclusion, we have successfully prepared the 2A4Y3S and 2A5Y2S frits using the melting method and investigated the effect of synthesis conditions on their phase transformation and physical properties. The glass transition temperatures (T_g) of the 2A4Y3S and 2A5Y2S samples were found to be 850 °C and 897 °C, respectively. The first crystallization temperatures (T_{c1}) occurred at 1120 °C and 1192 °C, while the second crystallization peak temperatures (T_{c2}) were observed at approximately 1284 °C and 1338 °C.

The eutectic temperatures were around 1302 °C and 1375 °C for the 2A4Y3S and 2A5Y2S frits, respectively. XRD and SEM analyses confirmed that the 2A4Y3S frit remained completely amorphous up to 800 °C, with maximum crystallization occurring between 1150 °C and 1200 °C. Above 1150 °C, the main crystalline phases observed were mullite, yttrium disilicate, and corundum.

In contrast, the 2A5Y2S frit remained completely amorphous up to 900 °C, with maximum crystallization occurring between 1250 °C and 1300 °C. Above 1250 °C, the primary crystalline phases included yttrium disilicate, yttrium silicate, corundum, and yttrium aluminum garnet. The prepared 2A4Y3S and 2A5Y2S frits show great potential for the fabrication of advanced SiAlON ceramics. Further optimization studies are ongoing and will be reported in future work.

Acknowledgments

The authors would like to express their gratitude for the research equipment support provided by the Institute of Chemistry and Material; Hanoi University of Science and Technology.

References

[1] Y. K. Kshetri, T. Kamiyama, S. Torii, S. H. Jeong, T.-H. Kim, H. Choi, J. Zhou, Y. P. Feng, and S. W. Lee, Electronic structure, thermodynamic stability and high-temperature sensing properties of Er-α-SiAlON ceramics, Scientific Reports, vol. 10, Mar. 2020. https://doi.org/10.1038/s41598-020-61105-z

[2] H. Mandal, N. C. Acikbas, Processing, characterization and mechanical properties of SiAlONs produced from low cost β-Si_3N_4 powder, KONA Powder Particle Journal, vol. 30, pp. 22-30, 2013.
https://doi.org/10.14356/kona.2013007

[3] F. Guo, Z. Yin, X. Li, J. Yuan, Spark plasma sintering of α/β-SiAlON ceramic end mill rods: electro–thermal simulation, microstructure, mechanical properties, and machining performance, Journal of Advanced Ceramics, vol. 12, iss. 9, pp. 1777-1792, Sep. 2023.
https://doi.org/10.26599/JAC.2023.9220786

[4] D. Hong, Z. Yin, F. Guo, and J. Yuan, Microwave synthesis of duplex α/β-SiAlON ceramic cutting inserts: Modifying m, n, z values, synthesis temperature, and excess Y_2O_3 synthesis additive, Journal of Advanced Ceramics, vol. 11, pp. 589602, Mar. 2022.
https://doi.org/10.1007/s40145-021-0559-x

[5] Y. K. Kshetri, B. Chaudhary, T.-H. Kim, H. S. Kim, S. W. Lee, Yb/Er/Ho-α-SiAlON ceramics for high-temperature optical thermometry, Journal of the European Ceramic Society, vol. 41, iss. 4, pp. 2400-2406, Apr. 2021.
https://doi.org/10.1016/j.jeurceramsoc.2020.12.006

[6] J. Huang, Y. Liu, M. Fang, Z. Huang, H. Li, S. Zhang, J. Yang, S. Huang, Synthesis and characterization of single-crystalline phase Li-α-SiAlON, Ceramics International, vol. 38, pp. 3391–3395, May 2012.
https://doi.org/10.1016/j.ceramint.2011.12.050

[7] N. Pradeilles, M. C. Record, D. Granier, R. M. Marin-Ayral, Synthesis of β-SiAlON: a combined method using sol–gel and SHS processes, Ceramics International, vol. 34, iss. 5, pp. 1189-1194, Jul. 2008.
https://doi.org/10.1016/j.ceramint.2007.02.017

[8] J. Marchi, D. S. Morais, J. Schneider, J. C. Bressiani, and A. H. A. Bressiani, Characterization of rare earth aluminosilicate glasses, Journal of Non-Crystalline Solids, vol. 351, pp. 863-868, Apr. 2005.
https://doi.org/10.1016/j.jnoncrysol.2005.01.078

[9] L. Wang, S. Fan, H. Sun, B. Ji, B. Zheng, J. Deng, L. Zhang, and L. Cheng, Pressure-less joining of SiCf/SiC composites by Y_2O_3–Al_2O_3–SiO_2 glass: Microstructure and properties, Ceramics International, vol. 46, iss. 17, pp. 27046-27056, Dec. 2020.
https://doi.org/10.1016/j.ceramint.2020.07.181

[10] H. Mao, M. Selleby, O. Fabrichnaya, Thermodynamic reassessment of the Y_2O_3–Al_2O_3–SiO_2 system and its subsystems, Calphad, vol. 32, iss. 2, pp. 399-412, Jun. 2008.
https://doi.org/10.1016/j.calphad.2008.03.003

[11] L. Granados, R. Morena, N. Takamure, T. Suga, S. Huang, D.R. McKenzie, and A. Ho-Baillie, Silicate glass-to-glass hermetic bonding for encapsulation of next-generation optoelectronics: a review, Materials Today, vol. 47, pp. 131-155, Jul-Aug, 2021.
https://doi.org/10.1016/j.mattod.2021.01.025

[12] B. He, G. Liu, J. Li, L. Wu, Z. Yang, S. Guo, and Y. Chen, Preparation of Y_2O_3–Al_2O_3–SiO_2 glasses by combustion synthesis melt–casting under high gravity, Materials Research Bulletin, vol. 46, pp. 1035-1038, Jul. 2011.
https://doi.org/10.1016/j.materresbull.2011.03.014

[13] A. C. Mendes, L.J.Q. Maia, E.C. Paris, and M. Siu Li, Solvent effect on the optimization of 1.54 μm emission in Er-doped Y_2O_3–Al_2O_3–SiO_2 powders synthesized by a modified Pechini method, Current Applied Physics, vol. 13, iss. 8, pp. 1558-1565, Oct. 2013.
https://doi.org/10.1016/j.cap.2013.06.012

[14] W. Zhu, H. Jiang, H. Zhang, S. Jia, and Y. Liu, Effect of TiO_2 and CaF_2 on the crystallization behavior of Y_2O_3-Al_2O_3-SiO_2 glass ceramics, Ceramics International, vol. 44, iss. 6, pp. 6653-6658, Apr. 2018.
https://doi.org/10.1016/j.ceramint.2018.01.076

[15] L. Zhang, L. Zhang, Z. Lin, Y. Jiang, J. He, W. Cai, and S. Li, Preparation of single phase nano-sized β-SiAlON powders by nitridation of silica–alumina gel in ammonia, Ceramics International, vol. 40, iss. 1, pp. 2539-2543, Jan. 2014.
https://doi.org/10.1016/j.ceramint.2013.07.064